Analyzing the Effect of Mid-Circuit Measurement on Spectator Qubits

Harshil Avlani

Abstract

Mid-Circuit Measurements (MCMs) are a key component in many quantum information algorithms. As such, ways to characterize their performance are of great interest. Specifically, it is important to determine what impact MCM has on nearby, unmeasured, spectator qubits. Here, I present a novel benchmarking analysis consisting of a variation of the Interleaved Randomized Benchmarking Technique. I use this method to evaluate MCM-induced spectator qubit error on various qubits inside IBM's quantum computer "ibm_oslo". I then examine the effect of qubit position on this error, test if IBM's widely-used quantum simulators account for this error, see how this error varies across different quantum computers, and posit potential causes of this error. This project has far reaching implications as it helps us beter understand a gate that will be integral to the advancement of quantum computing and discovers a deficiency with current IBM quantum simulators.

1 Introduction

Quantum computation holds significant potential as a computing paradigm beyond classical silicon-based computing. It offers immense advantages in efficiently solving problems such as integer factorization [1], combinatorial optimization [2], and quantum simulation [3] that are infeasible for classical computers. But so far, quantum computers have not shown any major, practical speedup over classical computers due to their high error rate and thus limited scalability. Due to this, it is almost universally accepted that for quantum computers to perform complex quantum algorithms with real world implications, some form of Quantum Error Correction (QEC) is necessary [4]. The quantum gate Mid-Circuit Measurement (MCM) is crucial to creating QEC algorithms, as most implementations of QEC require repeated stabilizer checks of ancilla qubits which encode information about errors that occurred during the execution of the circuit [5]. These checks allow for the real-time identification and eventual correction of errors. MCM also holds promise in creating more intricate post-selection schemes, which can support previously impossible experiments through a high level of simulated quantum control [6]. Additionally, when combined with the qubit reset gate, MCM provides the opportunity to leverage quantum computers more efficiently by reusing qubits, which is especially important in the current limited-qubit Noisy Intermediate Quantum (NISQ) era of quantum computing [5].

However, the hardware implementation of MCM makes it especially prone to errors. MCM involves sending a long duration microwave (which is required by nature of superconducting qubit measurement) to the measured qubit, which increases the chances that a pulse spillover occurs [7]. Pulse spillovers are a type of quantum cross-talk error where gate pulses perturb neighbouring spectator qubits in some way. It has previously been experimentally verified that MCM can leave a high residual cavity photon population on the measured qubit, and this could lead to pulse spillover error as the photons may cause unwanted coupling between the measured and spectator qubits [8]. Additionally, MCM has both classical and quantum ouputs, which could make MCM subject to error modes that do not exist for unitary quantum gates and terminating measurements (measurements that occur at the end of circuits) [8].

This study is a novel analysis into the effect of MCM on spectator qubits in superconducting quantum computers. Superconducting quantum computers were chosen as they are generally regarded as the most promising form of quantum computing and they are widely available through IBM Quantum [9, 16]. Similiar studies can be found in Ref. [11] and [10] In Ref [11], a variation of the benchmarking protocol presented in Section 2.1 is used to evaluate MCM-induced spectator qubit error in a trapped-ion quantum computer. However, since trapped-ion have completely different qubit construction and gate delivery methods, it is likely that the results of this study may not directly apply to superconducting quantum computers. Ref [10] also uses a similiar method to Section 2.1 to characterize MCM error in superconducting quantum computers, however this paper solely focuses on

the measured qubit.

2 Methods

2.1 Interleaved Randomized Benchmarking

Randomized Benchmarking (RB) is a technique to benchmark the performance of a quantum gate by estimating its average error rates over sequences of other randomly sampled gates [12]. For the context of this research, RB is preferable to other forms of error characterization (such as tomography) as RB doesn't require any state preparation and measurement (SPAM) [13]. Procedures for SPAM are generally error-prone, and thus it is difficult for SPAM-based characterization techniques to distinguish SPAM errors from errors caused by the quantum gate in question.

The specific RB protocol used is the Interleaved Randomized Benchmarking (IRB) protocol. IRB is a type of RB where the gate that we wish to characterize is interleaved between randomly constructed quantum gates [14]. Formally, the format for IRB can be written as

$$C_1, G, C_2, G, C_3, G, ..., C_{N-1}, G, C^\dagger$$

where each C_n represents a randomly constructed quantum gate, G represents the gate in question (in this case MCM), N represents the length of the IRB sequence (also called circuit length), and $C^\dagger$ represents the inverse of all prior C_n gates.

Since this research observes the effect of MCM on other qubits, it inherently requires a multi-qubit implementation of IRB. This means that the IRB gates get split such that all the G (MCM) gates are applied to the measured qubit while all the C_n and $C^\dagger$ gates are applied to the spectator qubits. A benefit of this is that MCM is performed repeatedly (N times) on the same qubit, which is similiar to how MCM would be used in real QEC algorithms. Thus, applying IRB in this manner will allow the benchmarking of the MCM gate in one of its most commonly used contexts. This paper only designates a single spectator qubit, as designating multiple spectator qubits opens the possibility to cross-talk error between spectator qubits as a result of the C_n gates, and it is extremely difficult to distinguish this error from MCM-induced error.

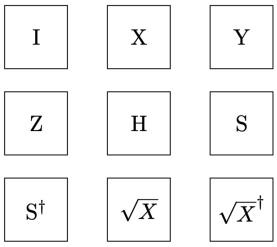

Figure 1: Quantum gates in the Clifford group that have been implemented on quantum computers

Single-qubit randomized Clifford gates were chosen as the randomly sampled quantum

gates for C_n. Clifford gates are composed of random subsets of the Clifford group, which are a group of quantum gates with the property that they always transform Pauli gates into other Pauli gates (Pauli gates are simply gates based on the Pauli matrices) [15]. This property is traditionally why Clifford gates have been widely used in randomized benchmarking, however, this logic doesn't apply here as MCM is not a Pauli gate. Instead, Clifford gates were chosen because they are essentially random groupings of commonly used quantum gates, which makes the C_n gates representatively simulate calculations on the spectator qubit. Clifford gates also have widespread compatability across many different quantum computers, which helps ensure that this benchmarking method is widely applicable [15].

2.2 MCM Circuit Construction

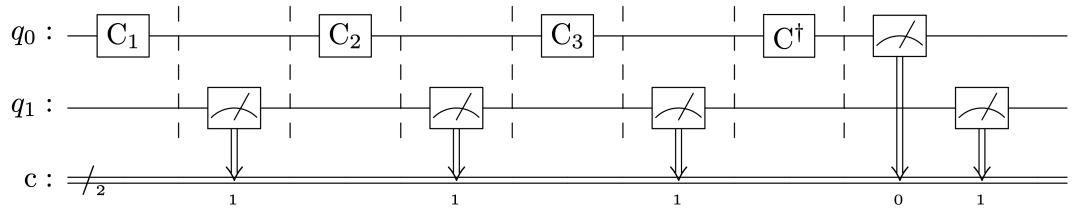

Figure 2: An example MCM circuit of length 4

The purpose of the MCM circuit is to characterize MCM-induced spectator qubit error with the IRB technique described in Section 2.1. This was done by applying the C_n and $C^\dagger$ gates to the spectator qubit (q_0) while applying the G gate (MCM) to the measured qubit (q_1). In the absence of error, q_0 will return to its starting state of $|0\rangle$ due to the fact that

$$|0\rangle \cdot C_1 \cdot C_2 \cdot C_3 \cdot ... \cdot C_{N-1} \cdot C^\dagger = |0\rangle$$

thus any measurement of $|1\rangle$ can be considered an error. It should be noted that the measured values from the MCM gates do not matter for this analysis, and in fact are overwritten by the terminating measurements.

2.3 Control Circuit Construction

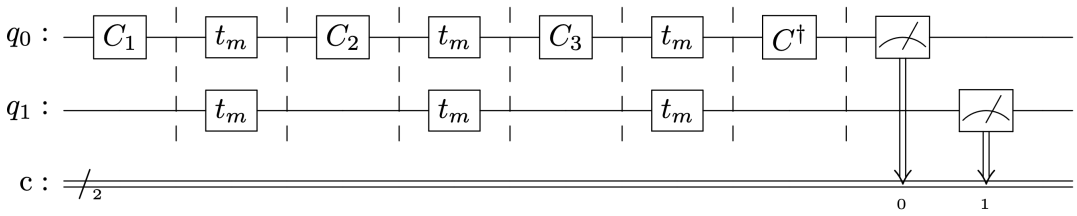

Figure 3: An example control circuit of length 4

However, it is important to note that the MCM gates are not the only source of error in quantum circuits. That is, even without the MCM gates, the MCM circuit would still have some error from the application of the Clifford and terminating measurements as well as environmental interaction. To account for this, a control circuit was created. The control circuit is functionally similiar to the MCM circuit in every way except that all the MCM gates are replaced by delays. These delays are of time t_m where t_m is equal to the time it takes the quantum computer to implement the MCM gate. This ensures that both circuits have the same duration, which controls for factors such as qubit exposure time. Similiarly to the MCM circuit, a measurement of $|1\rangle$ from q_0 can be considered an error.

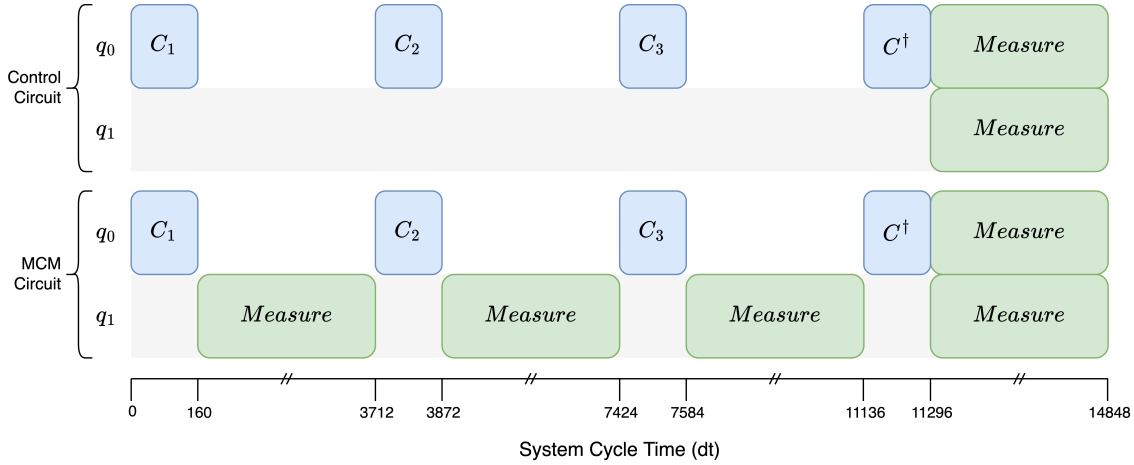

Figure 4: An example scheduling graph for a MCM and control circuit on ibm_oslo that shows equal circuit duration and gate execution times. Note dt is a variable unit that depends on the quantum computer.

2.4 Execution Protocol

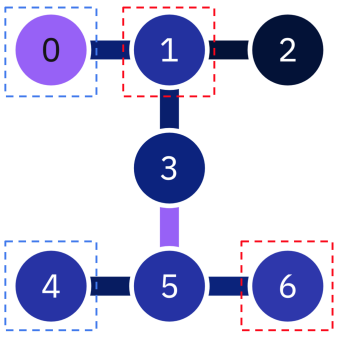

Figure 5: Qubit arrangement in ibm_oslo. Each circle represents a qubit. Red and blue boxes indicate qubits that were designated as spectators or measurement targets by the experiment (respectively). The connections between the qubits represent coupling channels. This image was created by IBM Quantum [16].

All circuits were created using the Qiskit quantum information library [17] and exe-

cuted on IBM's 7 qubit quantum computer ibm_oslo. The qubits that were designated as the spectator and measured qubit were varied within the quantum computer so the effect of spectator qubit proximity could be observed. Specifically, this experiment used 3 measured/spectator qubit pairs: 0/1, 0/6, and 4/6 respectively. These qubits were chosen due to the varying distances between them and low associated readout errors. A low readout

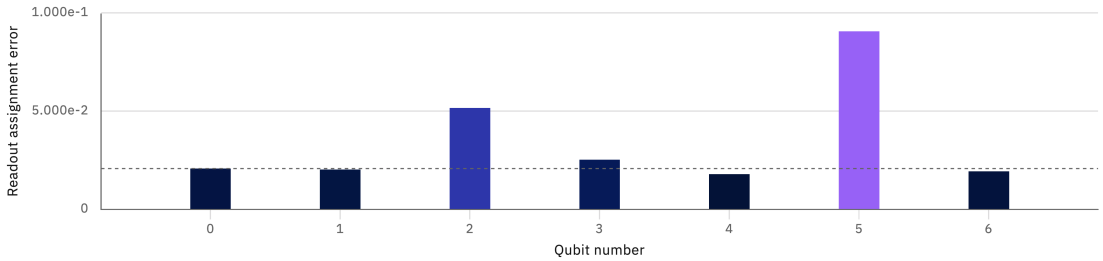

Figure 6: Graph of the readout error of ibm_oslo. The y axis represents the proportion of faulty measurements. These values were compiled by IBM using their calibration process. This image was created by IBM Quantum [16].

error means a more accurate reading of the state of the qubit at the end of the circuit, which allows for a better calculation of the spectator qubit error rate.

It should be noted that Figure 5 is to scale, and thus the neighbouring qubits in ibm_oslo (and the other IBM 7 qubit quantum computers used in Section 4) are equidistant from each other. This means that the distance between the qubit pairs can be standardized based on the number of coupling channels between them, as shown in Table 1, which will be useful for the analyses in Sections 3.2 , 3.3, and 4.

Qubit Pair	Distance
0/1	1
4/6	2
0/6	4

Table 1: Distances between qubit pairs in ibm_oslo

The MCM and control circuits were then generated from a length $N = 1$ to $N = 70$ for each measured/spectator qubit pair. Each of these circuits were then executed 3000 times, totalling 210,000 executions (70 sequentially generated circuits $\cdot$ 3000 execution per circuit) per type of circuit per qubit pair. Such a high number of executions is needed as quantum computers are inherently noisy, and thus to extract meaningful data from the benchmarking circuits for statistical analysis, a large sample size is neccesary. In each execution, the number of $|1\rangle$ measurements on the spectator qubit were recorded to measure the number of error instances on the qubit.

3 Results

3.1 Wilcoxon Signed-Rank Test

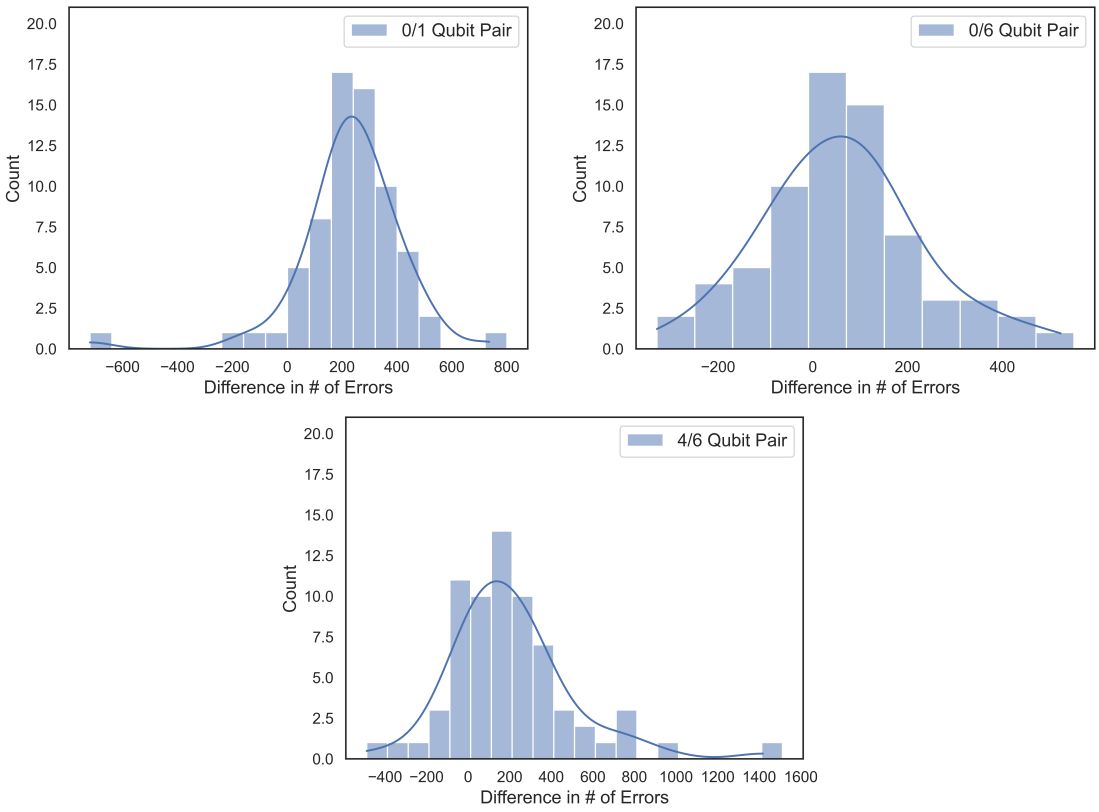

Figure 7: The histograms of the difference between the MCM and control circuit error counts for all 3 qubit pairs

A Wilcoxon test was conducted to see if the spectator qubit error rates significantly differed between the control and MCM circuit. Since the MCM and control circuits are identical except for the inclusion of MCM, any significant change between the error counts of the two can likely be attributed to MCM. The Wilcoxon test was chosen as it is non-parametric, which means that it doesn't assume normality. As seen in Figure 7, the error distributions of the 0/1 and 4/6 qubit pairs are likely not normal, which is confirmed by the Shapiro-Wilk normality test found in Table 1. The Wilcoxon test is a paired test, so

	p	Conclusion
0/1 Pair	3.997e-06	Not Normal
0/6 Pair	0.781	Normal
4/6 Pair	3.193e-04	Not Normal

Table 2: Results of the Shapiro-Wilk normality test. A significance level $\alpha = 0.05$ was used

the error counts of the MCM and control circuits wered paired based on circuit length to ensure a more meaningful comparison.

Circuit Length	1	2	3	4	5
MCM Circuit	847	880	410	999	1578
Control Circuit	1009	852	1129	750	1374

Table 3: First 5 entries of the MCM and Control circuit error count dataset for the 0/1 qubit pair. Shows how the error counts for the circuit are paired by circuit length

The null hypothesis H_0 is that there is no difference between the error rates distributions of the MCM and control circuit, and the alternate hypothesis H_a is that there is a difference between the error rates distributions of the MCM and control circuit.

	p	Conclusion
0/1 Pair	3.017e-11	Reject H_0
0/6 Pair	0.049	Fail to reject H_0
4/6 Pair	2.655e-06	Reject H_0

Table 4: Results of the Wilcoxon test

With a confidence level $\alpha = 0.01$, the 0/1 and 4/6 qubit pairs exhibited a significant difference in the error rates of the MCM and control circuit while the 0/6 pair did not. α was set as 0.01 to protect against the possibility of incorrectly rejecting H_0 as a result of the noisy output of the quantum computer. This shows that in some instances, MCM can cause a significant difference in spectator qubit error rate, however this effect is not uniform with qubit proximity. Additionally, the decreasing of the Wilcoxon test p values with increased qubit proximity suggests MCM's impact on spectator qubit may be heightened if the qubits are closer together.

3.2 Quade Analysis of Covariance (QANCOVA) Test

An QANCOVA test is a statistical test that evaluates the effect of some explanatory variable on some response variable while controlling for some covariate. This test was specifically chosen because it is non-parametric, which allows the standard normality assumption to be bypassed. The purpose of this test is to quantify the impact of qubit proximity on spectator qubit error rates, and this was done by designating the distance between qubits as the explanatory variable, the error counts of the repective qubit pair control circuit as the covariate, and the error counts of the respective qubit pair MCM circuit as the response variable. This makes it so that the QANCOVA test will remove the influence of the control circuit error on the MCM circuit error, thus allowing us to get a clearer sense of

p	η^2	SS
2.052e-07	0.1042	1.241e+06

Table 5: Results of the QANCOVA test

the effect of qubit proximity on the MCM circuit error. The fact that the p value is below any conceivable significance level suggests that qubit proximity has a significant effect on the MCM circuit error even after controlling for the control circuit error. Furthermore, the effect size η^2 tells us that 10.42% of the variance in the MCM circuit error is associated with qubit proximity, which shows that while qubit proximity is important, it is not the only significant factor contributing to MCM-induced spectator qubit error.

3.3 Graphical Analysis

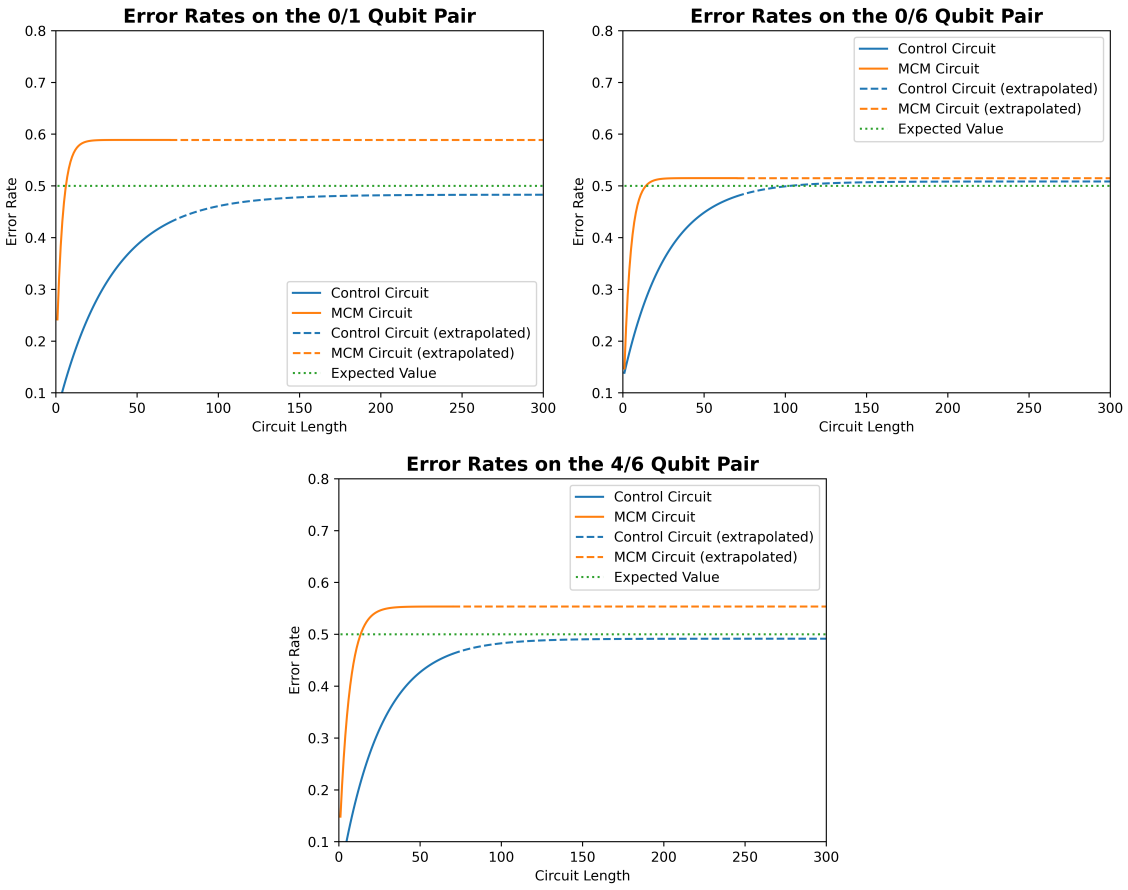

Figure 8: The error rate curves of the 3 tested qubit pairs from ibm_oslo

It would be expected that the error rate curves for each of the circuits should asymptote around a 50% error rate, as this constitutes a total random decision between the $|0\rangle$ and $|1\rangle$ states. From Figure 8, it can be seen that the control circuit error curves largely follow this

idea. However, the MCM circuits tend to asymptote at varying levels, with the 0/1 and 4/6 qubit pairs differing from the expected asymptote with decreasing magnitude. This means MCM-induced error affects spectator qubits in a non-random, correlated manner [18], which likely suggests that MCM-induced spectator error may be a direct result of spectator-measured qubit coupling as correlated quantum errors are usually associated with qubit interaction [19]. Another interesting thing to note from these graphs is that the MCM error curve reaches its asymptotic error rate much quicker (at a lower circuit length) compared to the control circuit, which indicates that MCM can significantly reduce the overall length at which the circuit is coherent. However, it is harder to specify any of these effect without a more intimate knowledge of the hardware topology of ibm_oslo, and this is not openly available.

In lieu of this, IBM's noisy Aer quantum simulator was checked to see if it accounted for this asymptote change seen in the 0/1 and 4/6 qubit pairs. Specifically, a Aer simulator was constructed with the same gate times, coupling map, and calibration data as ibm_oslo, to ensure a more equal comparison. From Figure 8, it can be seen that IBM's noisy quantum

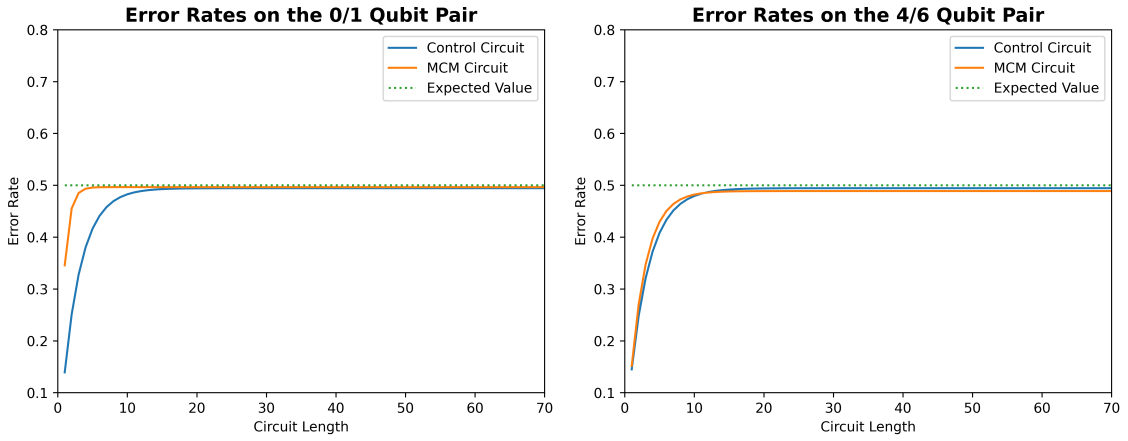

Figure 9: The error rate curves of the 2 qubit pairs that showed asymptote alteration on a simulator

simulators don't exhibit a clear asymptote change, which indicates that the simulators don't fully account for MCM-induced spectator qubit error. This is further shown by the fact that the circuit lengths at which the error curves reach their asymptotes are very different from the experimentally obtained values.

4 Macro Analysis

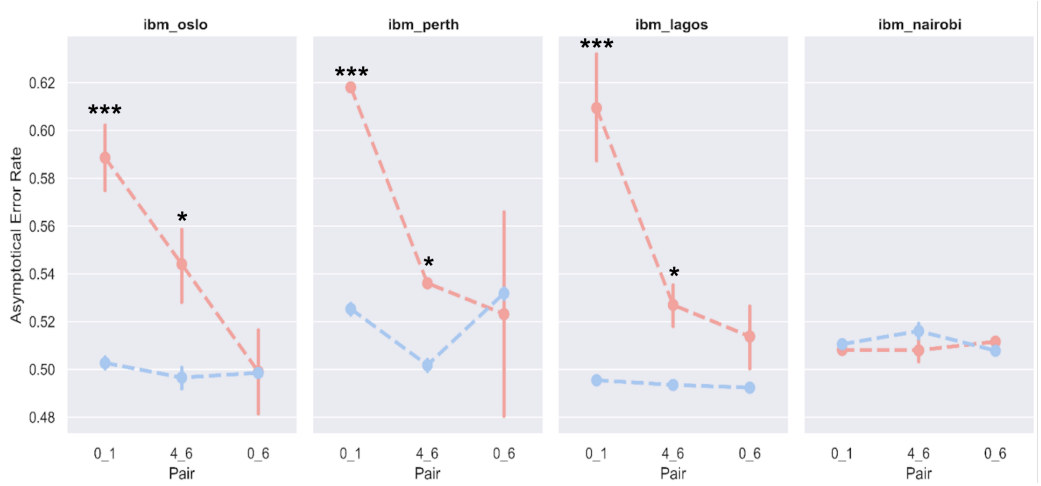

Figure 10: Graph of asymptotic error rate of the MCM circuit in different qubit pairs. Each point represents the mean of the error rate of multiple execution protocols. *** shows $p < 0.005$, ** shows $p < 0.01$, * shows $p < 0.05$. All p-values were determined by t-tests.

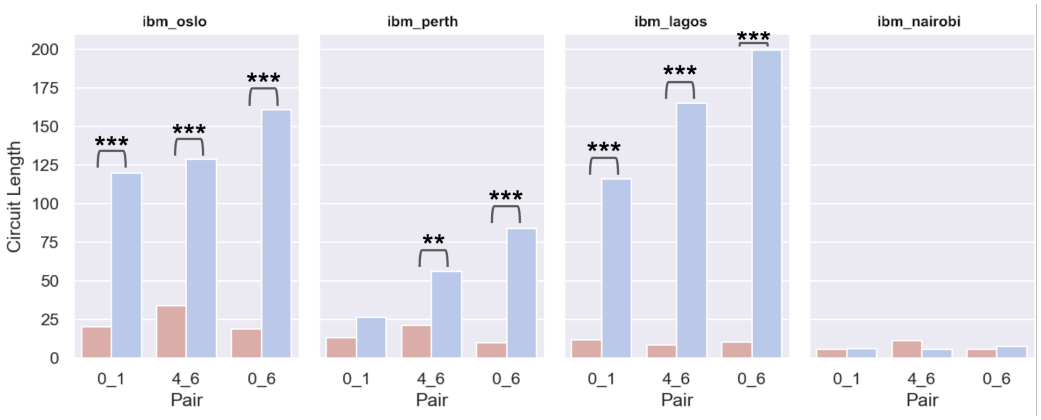

Figure 11: Graph of circuit length where asymptotic error rate of the MCM circuit is reached in different qubit pairs. Each bar represents the mean circuit length where asymptotic error was reached of multiple execution protocols. *** shows $p < 0.005$, ** shows $p < 0.01$, * shows $p < 0.05$. All p-values were determined by t-tests.

To analyze how MCM-induced spectator qubit error varied across difference quantum computers, the execution protocol described in Section 2 was applied to all 4 MCM-enabled 7 qubit quantum systems: ibm_oslo, ibm_perth, ibm_lagos, and ibm_nairobi. The number of succesful execution protocols on each qubit pair on each quantum computer is detailed in Table 6.

In total, 1,749 execution protocols were implemented in the macro-analysis, which is equivalent to roughly 367,000,000 circuit executions on quantum computers. The number of execution protocols for each qubit pair in each quantum computer was limited by quantum

	Control Circuit			MCM Circuit		
	0/1	4/6	0/6	0/1	4/6	0/6
ibm_oslo	62	94	94	37	53	38
ibm_perth	97	96	96	97	97	97
ibm_lagos	123	129	123	67	91	55
ibm_nairobi	62	63	66	5	2	5

Table 6: Number of succesful execution protocols for all tested qubit pairs and quantum computers.

computer availability as well as a data cleaning scheme. This data cleaning scheme ensured that only execution protocols with error curves that converged to some asymptote at a reasonable circuit length (a reasonable circuit length was defined as any circuit length $N < 250$) were used.

From Figure 10, it can be seen that ibm_oslo, ibm_perth, and ibm_lagos exhibited significantly different asymptotic error rates that scaled with qubit proximity. Additionally from Figure 11, it is evident that in ibm_oslo, ibm_perth, and ibm_lagos, the MCM circuit needed a significanly smaller circuit length to to reach its asymptotic error rate. This suggests that the inclusion of MCM in quantum circuits causes spectator qubit to reach their maximum error rate much quicker. ibm_nairobi likely didn't exhibit any of these findings because its error rate was too high (as seen by the extremely low circuit lengths in Figure 11) to find meaningful differences between the qubit pairs. It should be noted that ibm_nairobi is set to be retired on November 28th, 2023. From Figures 9 and 10, it can be seen that there is variance between quantum computers in asymptotic error rates and circuit lengths at which they are achieved, which may mean that MCM-induced spectator qubit error is affected by quantum computer-tunable factors, such as the qubit frequency, pulse amplitude, and T1/T2 coherence times.

5 Conclusion

This paper describes an analysis into the potential error that the quantum Mid-Circuit Measurement gate can cause on spectator qubits. To characterize this error, the Interleaved Randomized Benchmarking technique is used to create pairs of benchmarking circuits (one with MCM and one without) that are then run on various quantum computers. From the statistical tests described in Sections 3.1 and 3.2, it was concluded that MCM siginificantly increases spectator qubit error rates, and that this increase is partially associated with qubit proximity. As such, it is likely that reduced qubit proximity will reduce the magnitude of MCM-induced spectator qubit error. From a graphical analysis, it was found that the spectator qubits deviate from the expected error rate curve asymptote of 50%, which likely

indicates that MCM affects spectator qubits in a non-random manner. While comparing this to IBM's widely used Aer noisy quantum simulator suggested that quantum simulators do not properly account for the non-random manner of MCM-induced spectator qubit error. These findings were largely confirmed (by 3 of the 4 tested quantum computers) in the macro-analysis in Section 4, though there was variation between the quantum computers. Furthermore, from the analysis of circuit lengths in Section 4, it was found that MCM can cause the spectator qubit error rate to reach its max much quicker, confirming that MCM does indeed have a significant effect on spectator qubits.

This novel analysis into MCM-induced spectator qubit error has far-reaching implications and many avenues for further research. This research suggests that utilizing QEC algorithm that include MCM at high circuit lengths may end up adversely impacting the circuit, as MCM can cause significant spectator qubit error. This paper also finds that IBM's commonly used quantum simulators don't account for this error, and thus they need to be updated accordingly. Further research is needed to try to find other factors that may affect MCM-induced spectator qubit error, as qubit proximity is only associated with 10.42% of the variance in spectator qubit error. Other possible factors that may contribute to MCM-induced spectator qubit error include unintended coherent coupling between qubits, shared quantum environments, and possible shared classical environments. Additionally, the fact that MCM-induced spectator qubit error is dependent on qubit proximity could provide potential for quantum circuits to be spatially optimized to reduce MCM-induced spectator qubit error, though the practical efficacy of this needs to be tested. Lastly, it was suggested in Section 4 that MCM-induced spectator qubit error could be affected by quantum computer-tunable factors, so it might be possible to create a model to predict MCM-induced spectator error based on the calibration data of the quantum computer.

The main limitation to this project is the fact the the IRB method allows for the coarse detection of error, but to find the more intricate sources of error, it is likely a tomography-based approach is neccesary.

References

[1] Shor, P. W. (1997). Polynomial-Time Algorithms for Prime Factorization and Discrete Logarithms on a Quantum Computer. SIAM Journal on Computing, 26(5), 1484–1509. https://doi.org/10.1137/s0097539795293172

[2] Farhi, E., Goldstone, J., & Gutmann, S. (2014). A Quantum Approximate Optimization Algorithm. ArXiv:1411.4028 [Quant-Ph]. https://arxiv.org/abs/1411.4028

[3] Kassal, I., Jordan, S. P., Love, P. J., Mohseni, M., & Aspuru-Guzik, A. (2008). Polynomial-time quantum algorithm for the simulation of chemical dynamics. Proceedings of the National Academy of Sciences, 105(48), 18681–18686. https://doi.org/10.1073/pnas.0808245105

[4] Cai, W., Ma, Y., Wang, W., Zou, C.-L., & Sun, L. (2021). Bosonic quantum error correction codes in superconducting quantum circuits. Fundamental Research, 1(1), 50–67. https://doi.org/10.1016/j.fmre.2020.12.006

[5] Johnson, B. (2022, November 9). The full power of dynamic circuits to Qiskit Runtime. Retrieved from IBM Research Blog website: https://research.ibm.com/blog/quantum-dynamic-circuits

[6] Botelho, L., Glos, A., Kundu, A., Miszczak, J. A., Salehi, Ö., & Zimborás, Z. (2022). Error mitigation for variational quantum algorithms through mid-circuit measurements. Physical Review A, 105(2), 022441. https://doi.org/10.1103/PhysRevA.105.022441

[7] Rudinger, K., Hogle, C. W., Naik, R., Hashim, A., Lobser, D., Santiago, D., ... Young, K. (2021). Experimental Characterization of Crosstalk Errors with Simultaneous Gate Set Tomography. PRX Quantum, 2(4). https://doi.org/10.1103/prxquantum.2.040338

[8] Rudinger, K., Ribeill, G. J., Govia, L. C. G., Ware, M., Nielsen, E., Young, K., ... Proctor, T. (2021). Characterizing mid-circuit measurements on a superconducting qubit using gate set tomography. https://doi.org/10.48550/arXiv.2103.03008

[9] Foy, K. (2023, July 5). Superconducting qubit foundry accelerates progress in quantum research. https://news.mit.edu/2023/superconducting-qubit-foundry-accelerates-progress-quantum-research-0705

[10] Govia, L., Merkel, S. T., & McKay, D. C. (2022). A randomized benchmarking suite for mid-circuit measurements. ArXiv. https://doi.org/10.48550/arxiv.2207.04836

[11] Gaebler, J. P., Baldwin, C. H., Moses, S. A., Dreiling, J. M., Figgatt, C., Foss-Feig, M., ... Pino, J. M. (2021). Suppression of midcircuit measurement crosstalk errors with micromotion. Physical Review A, 104(6). https://doi.org/10.1103/physreva.104.062440

[12] Emerson, J., Alicki, R., & Życzkowski, K. (2005). Scalable noise estimation with random unitary operators. Journal of Optics, 7(10), S347–S352. https://doi.org/10.1088/1464-4266/7/10/021

[13] Magesan, E., Gambetta, J. M., & Emerson, J. (2011). Scalable and Robust Randomized Benchmarking of Quantum Processes. Physical Review Letters, 106(18). https://doi.org/10.1103/physrevlett.106.180504

[14] Magesan, E., Gambetta, J. M., Johnson, B. R., Ryan, C. A., Chow, J. M., Merkel, S. T., ... Steffen, M. (2012). Efficient Measurement of Quantum Gate Error by Interleaved Randomized Benchmarking. Physical Review Letters, 109(8). https://doi.org/10.1103/physrevlett.109.080505

[15] Grier, D., & Schaeffer, L. (2022). The Classification of Clifford Gates over Qubits. Quantum, 6, 734. https://doi.org/10.22331/q-2022-06-13-734

[16] IBM Quantum. https://quantum-computing.ibm.com/, 2023

[17] Qiskit Contributors. (2023). Qiskit: An Open-source Framework for Quantum Computing. https://doi.org/10.5281/zenodo.2573505

[18] Gaebler, J. P., Meier, A. M., Tan, T. R., Bowler, R., Lin, Y., Hanneke, D., ... Wineland, D. J. (2012). Randomized Benchmarking of Multi-Qubit Gates. Physical Review Letters, 108(26), 260503. https://doi.org/10.1103/PhysRevLett.108.260503

[19] Premakumar, V. N., & Joynt, R. (2018, December 17). Error Mitigation in Quantum Computers subject to Spatially Correlated Noise. https://doi.org/10.48550/arXiv.1812.07076